2024 NDIA MICHIGAN CHAPTER
GROUND VEHICLE SYSTEMS ENGINEERING
AND TECHNOLOGY SYMPOSIUM
POWER AND MOBILITY TECHNICAL SESSION
AUGUST 13-15, 2024 - NOVI, MICHIGAN

DETECTING DAMAGE USING ACOUSTIC EMISSION DURING EVALUATION OF HIGH-PRESSURE FUEL PUMP DURABILITY WITH LOW-VISCOSITY FUELS

Nikhil Murthy[1], Vincent Coburn[1], Caleb Matzke[1], Stephen Berkebile[1]

[1]U.S. DEVCOM Army Research Laboratory, APG, MD

ABSTRACT

This study looks at the effects of low-viscosity fuel on high-pressure fuel pump durability. Several high-pressure fuel pumps were allowed to operate with low-viscosity fuel on a custom test stand until failure. Fuel-pumps lasted 0.3-294 hours before failure. The fuel pumps failed by experiencing a sharp rise in the low-pressure outlet fuel temperature due to scuffing of the camring-bucket interface. We describe a technique for analyzing acoustic emission sensor data to monitor the status of the fuel pump. Acoustic emission signals were able to detect a two-stage failure process of scuffing initiation on a single camring-bucket interface to propagation of damage to the other interfaces.

Citation: N. Murthy, V. Coburn, C. Matzke, S. Berkebile, "High-Pressure Fuel Pump Low-Viscosity Fuel Durability Evaluation with Acoustic Emission Damage Detection," In *Proceedings of the Ground Vehicle Systems Engineering and Technology Symposium* (GVSETS), NDIA, Novi, MI, Aug. 13-15, 2024.

1. INTRODUCTION

High-pressure fuel pumps (HPFPs) are a critical component within high-pressure common rail diesel systems. The pumps generally use a cam driven plunger to pressurize the fuel at pressure up to 200 MPa to the common rail before injection into the engine. The pumps contain multiple sliding interfaces which rely on the pumped fuel for lubrication and are vulnerable to 'scuffing' wear.

Recent efforts to pursue alternative fuel sources such as sustainable aviation fuels (SAFs), ethanol or jet fuels pose a risk to the reliability of many vehicle systems. These alternative fuels have lower viscosity and lubricity than the diesel fuel most HPFPs are designed to use as shown by the ASTM fuel lubricity measurements shown in Table 1. The viscosity of fuel also decreases when operating in higher temperature environments, such as deserts. Fuel lubricity is influenced by many aspects both chemical and rheological [1]. The effect of low

Table 1. ASTM 5001 Ball on cylinder lubricity evaluator (BOCLE) Fuel Lubricity and viscosity of several fuels.

Fuel Name	Fuel Category	Viscosity at 40 °C (cSt)	BOCLE Wear Scar Diameter (µm)
DF-2	Diesel	2.52	464 ± 30
F-24	Jet Fuel	1.30	545 ± 12
ATJ	SAF	1.53	581 ± 4
Ethanol	N/A	1.10 [2]	593 ± 26
Decane	N/A	0.97 [3]	540 ± 66

viscosity fuels on fuel pump durability is unknown and is a goal of this study.

Another issue with fuel pump durability is the presence of multiple sliding interfaces, each vulnerable to failure and critical to the pump operation. Pumps can often be damaged on multiple interfaces complicating root-cause analysis.

One technique that has shown promise in diagnosis of failures is the use of high frequency acoustic emission (AE) sensors. Data from these sensors is often used in conjunction with power calculations, frequency analysis, position correlation or other signal processing tools [4-6]. The continuous wavelet transform is one example of a common signal processing tool used in time-frequency analysis.

This study determines the effect of low viscosity fuels on the durability of high-pressure fuel pumps. Additionally, it determines whether damage can be detected in a non-destructive manner using acoustic emission sensors coupled with a continuous wavelet transform for analysis.

2. PROCEDURES

Durability experiments were performed with a custom experimental test stand (shown in Fig. 1). The test stand was capable of independent control of four variables: rotation speed, input fuel temperature, high-pressure output pressure and high-pressure output flow rate.

Fuel started in the 20 L main tank. It was then pumped through an air/water filter and a 0.5 μm particle filter into an intermediate tank. The fuel was then drawn out of the intermediate tank through a heater, which regulates inlet fuel temperature, by the gear pump on the high-pressure fuel. The rotation speed of the pump was controlled by a variable frequency drive. The fuel then split into a low-pressure output and high-pressure output. The flow rate of the high-pressure output was regulated using the inlet metering

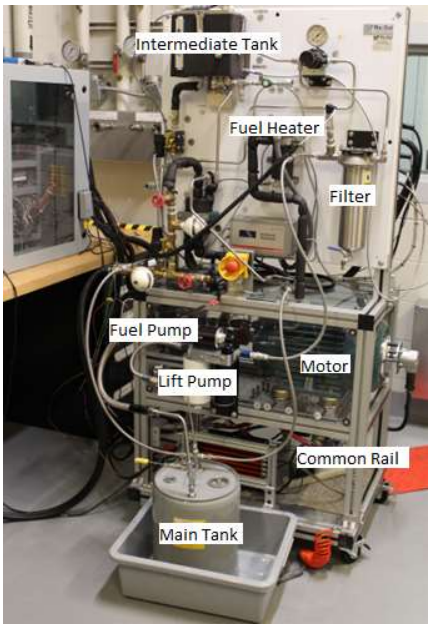

Figure 1: High-pressure fuel pump test stand

valve (IMV) on the fuel pump. The high-pressure output flowed into a common rail before flowing out of the common rail through its high-pressure valve (HPV), which both regulated the pressure in the high-pressure fuel lines and reduced the pressure of the fuel downstream. The low-pressure fuel exiting the HPV was cooled and combined with the low-pressure output of the fuel pump then moved through addition chillers and filters before returning to the main tank.

The test stand had a number of sensors monitoring the status of the fuel pump. Thermocouples were mounted in the inlet and return fuel lines and surface mounted to the fuel pump. Flow meters measured the inlet fuel and high-pressure output flow rates. Two sensors measured the pressure of the high-pressure fuel. One sensor was located in the common rail and used for pressure control. The second pressure sensor was mounted in the fuel pump immediately outside the outlet valve of one of the plunger bores. The rotational position of the main shaft was measured with a rotary encoder.

Lastly, an acoustic emission sensor, sensitive to 50-500kHz vibrations, was mount on the pump housing and used for the diagnostic methods described below. The location of the sensor guarantees that the fuel pump is the primary source of the signal.

The test article used in the experiments had a widely used fuel pump design of a trigonal camring with plunger-bore compression. This pump design has a series of plungers driven by a central camshaft. The camshaft has a central camring, which translates in a circular motion against a bucket tappet. The bucket interfaces with a plunger inside a tightly machined bore which draws fuel from an inlet valve and compresses it out through an outlet valve toward the high-pressure output of the pump. The pump has three identical plunger-bores each with its own bucket, plunger, valves a corresponding face of the camring. Figure 2 shows an example of the various sub-components.

The durability test started by first performing a break-in procedure using F-24 jet fuel. During the break-in, the operating speed and pressure were slowly increased over 1 hour until they reach 2000 RPM and 1400 bar. The flow rate was maintained at 770 mL/min and the inlet fuel temperature at 40 ºC. The fuel pump was then run for 24 hours. After the break in the F-24 fuel was drained from the test stand and flushed out with one of the desired test fuels. Two test fuels were used for our experiments, ethanol and decane. Both ethanol and decane have a viscosity of ~1 cSt. A total of five experiments were run, three with ethanol and two with decane. After switching to the desired test fuel, the pump was run at 2000 RPM, 1400 bar, 770 mL/min and 40 ºC, until one of the failure criteria was reached. The failure criteria were either an increase or reduction in pressure, flow rate or temperature set by a simple threshold.

After failure, the fuel pump was disassembled, and the sub-components were analyzed for damage. The components were photographed and imaged using a brightfield optical microscope. Components with visible damage were also imaged with a scanning electron microscope (SEM) with additional elemental analysis using electron dispersive spectroscopy (EDS).

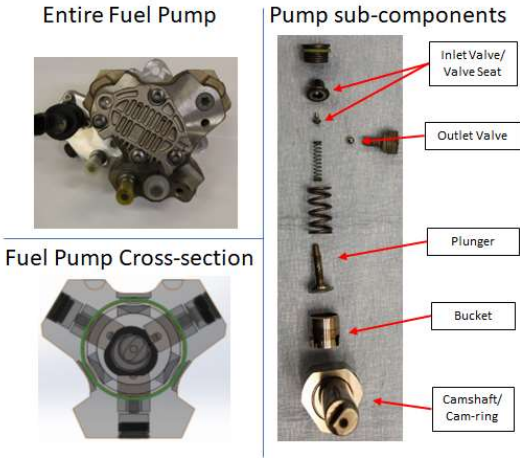

Figure 2: High-pressure fuel pump cross-section and sub-components

3. DATA ANALYSIS

Acoustic emission data taken during the experiments was post-processed to determine the status of the pump during the experiment. The acoustic data was record in short bursts, 0.2 s in length, with an interval of 10-30 s at a data acquisition rate of 1 MHz. This results in a single burst of data having 200,000 data points as shown in Fig. 3a. Additionally, the root-mean-squared (RMS) of the acoustic emission intensity was collected every 1 sec.

A continuous wavelet transform was used on each burst of data transforming the time series intensity data into time-frequency intensity data. The time-frequency data was then combined with rotary encoder data to correlate the average intensity with angular position resulting in position-frequency intensity data as seen in Fig. 3b. Lastly, each burst acquisition was time-stamped. Compiled together the acoustic data can be represented as a single three-dimensional

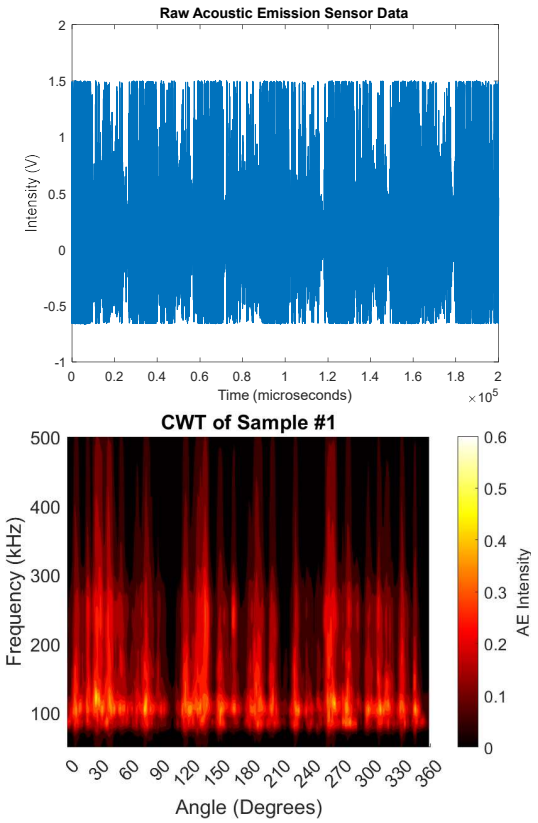

Figure 3: Acoustic emission signal data: Raw (a) and after position-frequency intensity analysis (b)

matrix of intensity as a function of time, frequency, and angular position for the entire experiment.

4. RESULTS AND DISCUSSION

The fuel pumps had a lifetime ranging from 0.3 to 294 hours for the five pumps in our experiment as summarized in Table 2. There are two significant observations about these lifetimes. First, the fuel pumps operating with these low-viscosity 1 cSt fuels have much lower lifetimes than expect from fuel pumps operating with diesel, which can typically exceed 3000 hours. The second observation is that the variance in lifetime is quite high, with the two tests in decane having a ~100 times difference. Due to the large variance and low sample size, no statistically significant difference between the two fuels could be observed.

Table 2. Lifetime of fuel pumps with low-viscosity fuel.

Experiment #	Test Fuel	Lifetime (Hours)
1	Ethanol	0.3
2	Ethanol	151.2
3	Ethanol	43.1
4	Decane	3.1
5	Decane	294.4

The remainder of the paper focuses on two specific tests, one for each fuel, to provide an example of the observations seen in all the pumps.

In our example decane experiment, the fuel pump operated for 3.085 hours before failing by exceeding the low-pressure outlet fuel temperature limit of 80 °C as shown in Figure 4a. All thermocouples showed a similar pattern in temperature, but the low-pressure outlet fuel temperature shows the largest change. Looking closely at the temperature,

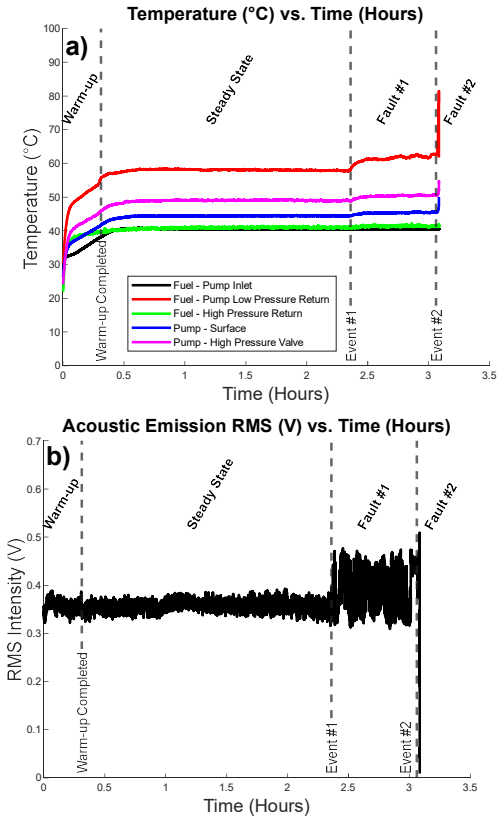

Figure 4: Temperature (a) and acoustic emission RMS intensity of a fuel pump run with decane

it a distinct pattern corresponding to different states of operation can be observed. The temperature first started to rise during a warm-up period when the test stand turned on before reaching a steady-state condition of 58 °C. A small increase in temperature to 61 °C after 2.4 hours of operation was then observed, which will be called failure event #1. The temperature then stabilized before a second, much larger temperature increase at 3.0 hours until it reached the abort limit of 80 °C, which will be called event #2. Increases in acoustic emission RMS intensity were observed to correspond to the temperature increases at event #1 and event #2 as shown in Fig 4b. We can define four states of the pump defined by these events: warm-up, steady-state, fault #1, and fault #2 as shown in Fig 4.

Figure 5: Photographs (left) and brightfield optical images (right) of damaged fuel pump sub-components from experiment with decane.

Scuffing wear of the camring and bucket surfaces corresponding to all three plunger bores was observed, upon tear-down of the fuel pump in the decane experiment. Figure 5 shows photographs of the scuffed camring and bucket surfaces. The scuffing wear on the camring occurred primarily where the camring and bucket contact each other during the output stroke of the plunger, which is when the pressure in the contact is highest. There was scuffing on both the top surface of the bucket, which contacts the camring, and the side surfaces, which contact the pump housing. Under normal operation, the bucket-housing interface is not loaded, but we believe wear of the camring-bucket interface may cause misalignment of the components and excessive loading of other related interfaces.

Chemical analysis of the scuffed surfaces leads us to believe a low-oxidization scuffing process is responsible for the component

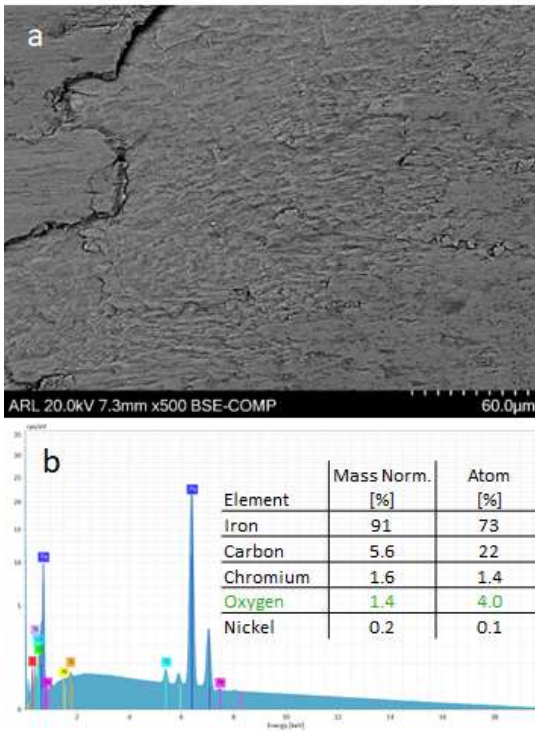

Figure 6: Backscatter SEM images (a) and EDS elemental analysis of a damaged camring after operating with decane.

wear. Figure 6 shows SEM and EDS measurements of the camring. The topography of the surface shown in the image is typically of scuffing. The surface had large cracks where the wear debris has broken away along with plastic deformation of the surface giving a smeared appearance. The EDS spectra shows oxygen concentrations 4 at% or less, which indicates very low levels oxide film formation. There is no significant difference between oxygen concentration in the scuffed surface versus the non-scuffed surface.

The acoustic emission data gives insight into what happened during the two events preceding failure of the pump. The data analysis techniques described in section 3 of this paper were applied to acoustic emission data collected during the decane experiment. Figure 7 shows an example of the resulting position-frequency intensity plots at three of the four states of the pump. Minor difference exist between the acoustic data between the warm-up and steady-state operating. However after event #1, the formation of a large band in intensity between 60° and 150º for the crank angle is observed. After event #2 there are three bands at 30°, 150º, and 270°.

There are a number of conclusions that can be made from interpreting the position-frequency intensity plots. Firstly, the position-frequency analysis is able to clearly distinguish between different states of the pump. Second, the acoustic emission signal gives us information about where the damage occurred. The pump has a three-fold symmetry, which can be seen clearly in the fault #2 acoustic data where three bands of intensity are spaced 120º apart. The three bands correspond to the three separate camring-bucket interfaces, which were found to be damaged from the tear-down analysis. The last conclusion that can be made is that the fuel pump has two stages of failure: 1) An initiation stage where scuffing occurs for one of the three camring-bucket interfaces and 2) a propagation stage where damage spreads to other interfaces in the pump. There is evidence of this from the acoustic signal, where the formation of a single band of intensity after event #1 corresponds to damage initiation and the formation of three bands to the damage propagation.

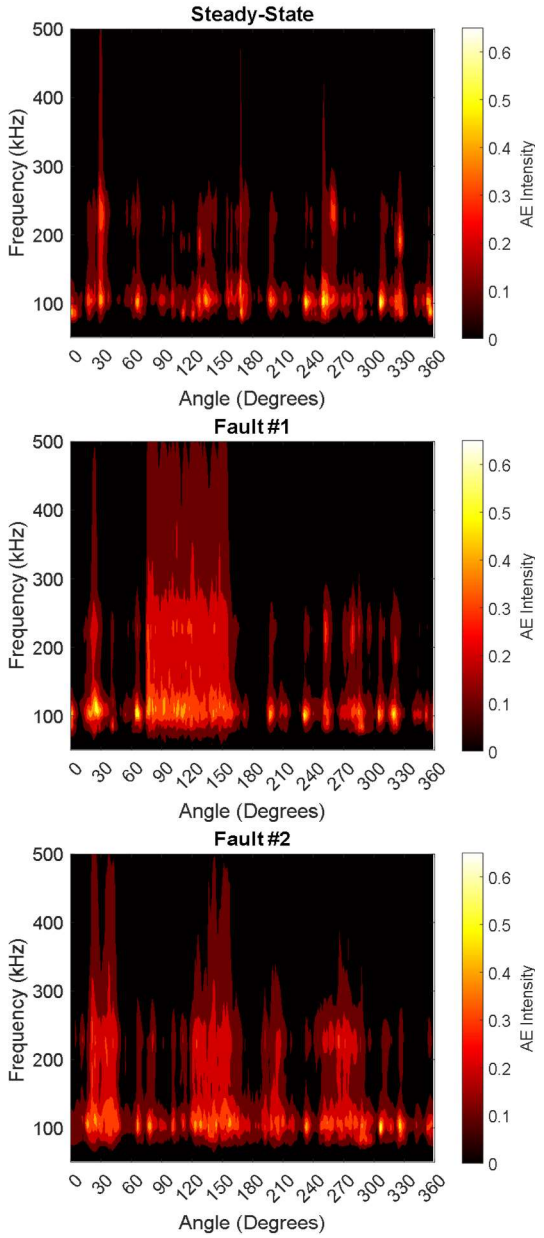

Figure 7: Acoustic emission time-frequency intensity during three different states of operation.

Finally, we will briefly summarize the results of a separate experiment with ethanol. Our example ethanol test lasted for 43.1 hours before exceeding the limit for the low-pressure outlet fuel temperature. Most of the fuel pumps failed for this reason. Similar to the decane pump, scuffing was also observed on all three camring-bucket interfaces. The scuffing had low oxidation just like the decane experiment, but for ethanol more severe damage of the surfaces was observed. The ethanol experiment saw a similar increase in the temperature and acoustic emission at two distinct events, similar to the decane experiment. The ethanol experiment also showed the formation of a single band of intensity after event #1 followed by two more bands following event #2. One key difference is that for the ethanol experiment the two events occurred only 30 s apart as opposed to the 0.6 hour gap for our decane experiment, despite the fact that the total duration of experiment was much longer, 43.1 hours for the ethanol test vs. 3.0 hours for the decane experiment. This shows that there is a high variance in the time when both events occur that is independent of the total durability. The last observation is that the position-frequency data varied slightly for all the experiments meaning that pump-to-pump variations must be considered when comparing data from different fuel pumps.

It is important to note some key differences between the experiments in this paper and fuel pumps used in real applications. First, all of our fuel pumps were operated at fixed conditions for rotation speed, pressure, flow rate and fuel temperature. In an engine all four parameters are variable. Additionally, our sensors are not subjected to the vibrations generated from the rest of the engine, which could complicate interpretation of the signal in real applications and require more sophisticated models or processing techniques. It is important to note that while simple methods for determining the pump status, such as tracking the temperature or acoustic emission RMS may be predictive in the test stand, these values may vary much more greatly in a real application.

5. CONCLUSIONS

Several experiments were run to test the durability of high-pressure fuel pumps when operating with low-viscosity fuels. From these experiments the following conclusions can be made:

- Fuel pump durability is significantly lower when operating with low-viscosity fuel than diesel.
- The fuel pumps failed due to non-oxidative scuffing of the bucket-camring interface.
- The failure resulted in a rise in the low-pressure output fuel temperature.
- The fuel pumps failed in two stages: damage initiation and damage propagation.
- Position-frequency processed acoustic emission signals are able to detect the two stages of failure.
- There is a large variance in the time to damage initiation, propagation, and total time to failure.

6. REFERENCES

[1] P.Y. Hsieh, T.J. Bruno, “A perspective on the origin of lubricity in petroleum distillate motor fuels,” Fuel Processing Technology, vol 129, pages 52-60, 2015

[2] F.A.M.M. Goncalves, A.R Trindade, C.S.M.F. Costa, J.C.S. Bernardo, I. Johnson, I.M.A. Fonseca, A.G.M. Ferreira, “PVT, Viscosity and Surface Tension of Ethanol: New Measurements and Literature Data Evaluation,” The Journal of Chemical Thermodynamics, vol 42, issue 8, pages 1039-1049, 2010

[3] E.W. Lemmon, I.H. Bell, M.L. Huber, M.O. McLinden, “Thermophysical

Properties of Fluid Systems" in *NIST Chemistry WebBook, NIST Standard Reference Database Number 69*, Gaithersburg, MD, Accessed: 02/15/2024 [Online]. Available: https://webbook.nist.gov/chemistry/fluid/

[4] A. Bejger, J. B. Drzeweineicki, "The Use of Acoustic Emission to Diagnosis of Fuel Injection Pumps of Marine Diesel Engines," Energies, vol 12, issue 4661, 2019.

[5] B. Dykas, J. Harris, "Acoustic Emission Characteristics of a Single Cylinder Diesel Generator at Various Loads and with a Failing Injector", Mechanical Systems and Signal Processing, vol 93, pages 397-414, 2017.

[6] B. V. Van Hecke, J. Yoon, D. He, "Low Speed Bearing Fault Diagnosis Using Acoustic Emission Sensors", Applied Acoustics, vol 105, pages 35-44, 2016